Oncogene (2001) 20, 1254–1265

www.nature.com/onc

Caspase-mediated Cdk2 activation is a critical step to execute transforming growth factor-β1-induced apoptosis in human gastric cancer cells

Sang Gyun Kim[1,2], Se Nyun Kim[2], Hyun-Soon Jong[1], Noe Kyeong Kim[3], Seung Hwan Hong[2], Seong-Jin Kim[4] and Yung-Jue Bang*[,1,3]

[1]*Cancer Research Institute, Seoul National University College of Medicine, Seoul 110-744, Korea;* [2]*School of Biological Sciences and Institute for Molecular Biology and Genetics, Seoul National University, Seoul 151-742, Korea;* [3]*Department of Internal Medicine, Seoul National University College of Medicine, Seoul 110-744, Korea;* [4]*Laboratory of Cell Regulation and Carcinogenesis, National Cancer Institute, Bethesda, Maryland, MD 20892-5055, USA*

Although TGF-β1, a growth inhibitor, is known to also induce apoptosis, the molecular mechanism of this apoptosis is largely undefined. Here, we identify the mechanism of TGF-β1-induced apoptosis in SNU-16 human gastric cancer cells. Cell cycle and TUNEL analysis showed that, upon TGF-β1 treatment, cells were initially arrested at the G1 phase and then driven into apoptosis. Of note, caspase-3 was activated in accordance with TGF-β1-induced G1 arrest. Activated caspase-3 is targeted to cleave p21^{cip1}, p27^{kip1}, and Rb, which play important roles in TGF-β-induced G1 arrest, into inactive fragments. Subsequently, Cdk2 was aberrantly activated due to the cleavage of p21 and p27. We found that the inhibition of Cdk2 activity efficiently blocks TGF-β1-induced apoptosis, whereas it did not prevent caspase-3 activation or the subsequent cleavage of target proteins. In contrast, the suppression of caspase-3 activity inhibited the cleavage of target proteins, the activation of Cdk2, and the induction of apoptosis. Taken together, our results suggest that activation of caspase-3 by TGF-β1 may initiate the conversion from G1 cell cycle arrest to apoptosis via the cleavage of p21, p27 and Rb, which in turn causes Cdk2 activation and, most significantly, Cdk2 activation as a downstream effector of caspase is a critical step for the execution of TGF-β1-induced apoptosis. *Oncogene* (2001) **20,** 1254–1265.

Keywords: TGF-β1; apoptosis; caspase-3; cyclin-dependent kinase 2; p21^{cip1}; p27^{kip1}

Introduction

Transforming growth factor-β1 (TGF-β1), a multifunctional polypeptide, has been shown to inhibit cellular proliferation by cell cycle arrest or apoptotic cell death (Roberts and Sporn, 1990; Kingsley, 1994). The mechanism of TGF-β1-mediated growth arrest at the G1 phase in epithelial cells includes the inhibition of cyclin D, E and A mRNA expressions (Ko *et al*., 1995; Slingerland *et al*., 1994; Geng and Weinberg, 1993), a reduction of cyclin-dependent kinase 4 (Cdk4) synthesis (Ewen *et al*., 1993), and a down-regulation of Cdk2 kinase activity (Koff *et al*., 1993; Reynisdottir *et al*., 1995). In addition, Cdk inhibitors, namely p15^{ink4} (p15), p21^{cip1} (p21), and p27^{kip1} (p27), have been reported to be potential cellular mediators in TGF-β1-induced cell cycle arrest (Datto *et al*., 1995; Hannon and Beach, 1994; Polyak *et al*., 1994). The induction or redistribution of these molecules by TGF-β1 effectively suppresses the activity of the G1 cyclin/Cdk complex, and hence, this is considered as a hallmark of the TGF-β1-mediated growth inhibitory effect. In addition, retinoblastoma protein (Rb) has been implicated as a target of TGF-β1-induced negative signals (Laiho *et al*., 1990, Pietenpol *et al*., 1990) because the TGF-β1-induced accumulation of hypophosphorylated Rb prevents progression into the S phase. These effects on Rb are postulated to be derived from the inhibition of Cdk activity by TGF-β1 toward Rb (Ewen *et al*., 1993; Koff *et al*., 1993).

More recently, TGF-β1 has been found to elicit cell death in various transformed cells. However, the molecular mechanism by which TGF-β1 exerts its apoptotic effect is not fully understood. Some reports have suggested that the activation of caspase family proteases (Chen and Chang, 1997; Choi *et al*., 1998; Schrantz *et al*., 1999), the involvement of oxidative processes (Sánchez *et al*., 1996), the down-regulation of Bcl-2 (Lafon *et al*., 1996) and the inhibition of Rb gene expression (Fan *et al*., 1996) could each be postulated to play a role in TGF-β1-induced apoptosis.

To date, TGF-β1-induced G1 arrest and apoptosis have been studied separately because they were associated with different phenomena and believed to be separate cellular mediators. However, it is intriguing that apoptosis may be linked to G1 arrest under some circumstances (Meikrantz and Schlegel, 1995; King and Cidlowski, 1995). This raises the possibility that

*Correspondence: Y-J Bang, Department of Internal Medicine, Seoul National University College of Medicine, 28 Yongon-dong, Chongro-gu, Seoul 110-744, Korea
Received 22 August 2000; revised 14 December 2000; accepted 19 December 2000

molecules whose activities facilitate execution of the apoptotic process may be activated in the G1 phase. Progression through G1 and entry into the S phase is regulated by Cdk2, which is controlled by cyclins and Cdk inhibitors (Hunter and Pines, 1994; Sherr and Roberts, 1999), which implies that these molecules may also be involved in the apoptotic process. Indeed, recent observations have shown that the overexpression of cyclins (Fotedar *et al*., 1995) and the aberrant activation of cyclin-dependent kinases, including Cdk2, are closely linked to apoptosis in many experimental systems (Park *et al*., 1996; Meikrantz and Schlegel, 1996; Levkau *et al*., 1998; Hakem *et al*., 1999; Harvey *et al*., 2000). Thus, we hypothesized that the cellular mediators involved in TGF-β1-mediated growth arrest are also associated with TGF-β1-induced apoptosis.

In the present study, we examined the participation of cell cycle regulatory proteins in the process of the TGF-β1-induced apoptosis of SNU-16 cells. We found that the conversion from growth arrest to apoptosis by TGF-β1 was initiated by activated caspase-3, which induces the cleavage of p21, p27, and Rb and subsequent Cdk2 activation. Most importantly, we provide evidence that aberrantly elevated Cdk2 activity, as an essential downstream effector of caspase, drives TGF-β1-treated cells into irreversible apoptotic cell death.

Results

TGF-β1 triggers initial G1 cell cycle arrest and subsequent G1 phase specific apoptosis in SNU-16 cells

SNU-16 is a poorly differentiated gastric cancer cell line that is very sensitive to TGF-β1 (Park *et al*., 1990, 1994). To test whether its sensitivity to TGF-β1 is caused by G1 arrest and/or apoptosis, we first analysed the cell cycle distribution by examining the cellular DNA content. When cells were treated with 5 ng/ml of TGF-β1, the population of both G1 and G2/M phases slightly increased for an initial 12 h and thereafter decreased, whereas the S phase population declined progressively (Figure 1a). The population of the sub-G1 cells slightly increased until the 12 h, and subsequently increasing dramatically after 24 h (Figure 1a). These results show that TGF-β1 induces apoptotic cell death in SNU-16 cells. We confirmed apoptotic cell death with other markers of apoptosis such as a chromosomal ladder formation (Figure 1b), a phosphatidylserine externalization (Figure 1c), and the characteristic morphological changes such as cell shrinkage and cytoplasmic blebbing in TGF-β1-treated cells (data not shown).

Since TGF-β1 has been known to be a potent growth inhibitor (Alexandrow and Moses, 1995), we next examined whether TGF-β1-mediated G1 cell cycle arrest is a prerequisite for apoptosis in SNU-16 cells. To this end, at different time points after TGF-β1 treatment, cells were double-stained with terminal deoxythymidine transferase-mediated dUTP nick end labeling (TUNEL) for apoptosis and propidium iodide (PI) for cell cycle distribution and analysed by flow cytometry (Figure 2a). After 12 h incubation with TGF-β1, G1 cells (2N DNA contents) began to increase and TUNEL-positive (apoptotic) cells slightly increased from the population of G1 phase cells at this time point. Twenty-four hours after treatment with TGF-β1, TUNEL-negative (non-apoptotic) cells at the S/G2/M phase (>2N DNA contents) moved into the G1 phase and, at the same time, a dramatic increase in TUNEL-positive cells was observed in the cells at the G1 phase rather than at the S/G2/M phase. After 48 h, the majority of cells had moved into the TUNEL-positive area (Figure 2a). These results suggest that, upon TGF-β1 treatment, cells are initially arrested at the G1 phase and apoptosis specifically occurs in cells at this phase. To confirm these, we additionally performed the pulse labeling of cells with BrdU for 1 h before they were harvested for flow cytometry analysis. The bivariate analysis with DNA content and BrdU staining are shown in Figure 2b. After treatment with TGF-β1, BrdU-positive cells (S phase cells) significantly declined in a time-dependent manner and cells were accumulated at the G1 phase suggesting that TGF-β1-treated cells are arrested at the G1 phase of the cell cycle before the induction of apoptosis. In addition, after 24 h incubation with TGF-β1, the sub-G1 cells dramatically increased in the BrdU-negative area indicating that apoptotic cell death is induced at the G1 phase, not at the early S phase. The fact that TGF-β1-induced G1 arrest occurs in SNU-16 cells was also confirmed by another analysis of cell cycle distribution that the proportion of G1 phase cells increased time-dependently in viable non-apoptotic cells (⩾2N DNA contents) (Figure 2c). Therefore, a progressive decline of S phase cells (Figure 1a) resulted from the blockade of the G1-S transition by TGF-β1-mediated G1 arrest. In addition, 24 h after stimulation with TGF-β1, the relatively small decrease of cells at the G1 phase, compared to the observed increase of apoptotic cells (Figure 1a), was caused by the accumulation of G1 phase cells from the S/G2/M phase by cell cycle progression.

Apoptosis induced by TGF-β1 is dependent on the activation of caspase-3

To examine the mechanism of the G1 phase-specific induction of apoptosis by TGF-β1, we next investigated the involvement of caspase activation. Since caspase-3-like proteases are the major caspases activated in response to distint apoptosis-inducing stimuli (Patel *et al*., 1996; Faleiro *et al*., 1997), we examined whether caspase-3 is activated during TGF-β1-induced apoptosis. As shown in Figure 3a, the inactive 32 kDa proform of caspase-3 decreased after TGF-β1 treatment, which was associated with the appearance of fragments of caspase-3. The p17 and p19 fragments of caspase-3 were initially detected 12 h after stimulation with TGF-β1, and the amount of the active p17 fragment gradually increased until the 48 h

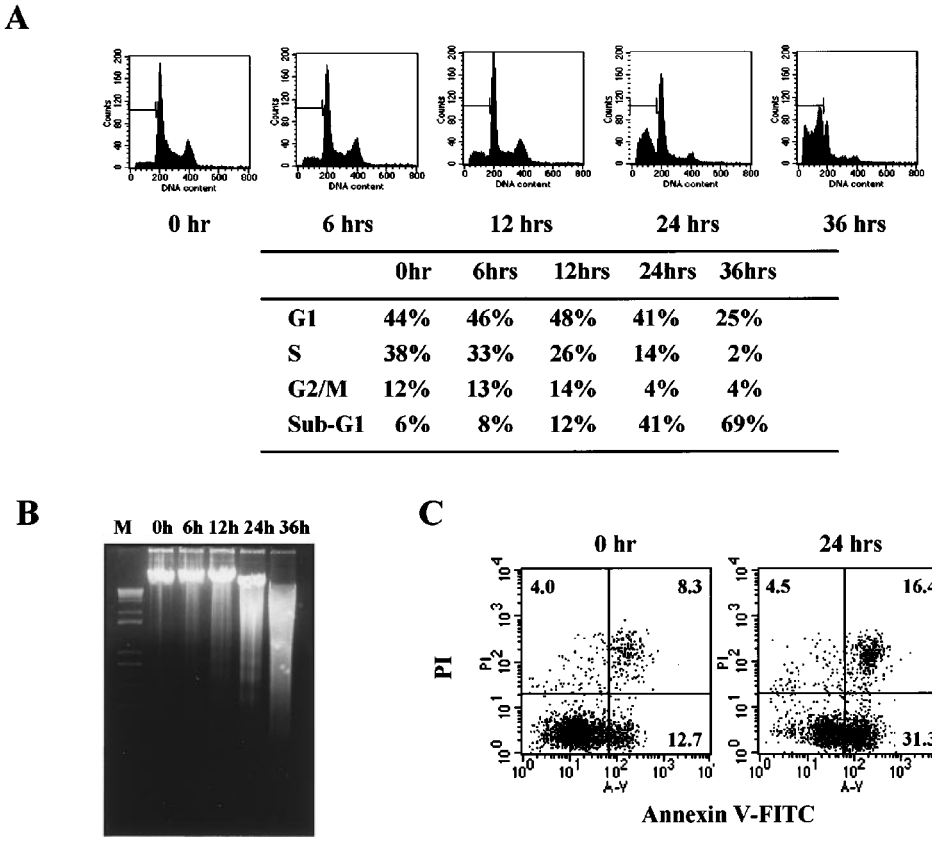

	0hr	6hrs	12hrs	24hrs	36hrs
G1	44%	46%	48%	41%	25%
S	38%	33%	26%	14%	2%
G2/M	12%	13%	14%	4%	4%
Sub-G1	6%	8%	12%	41%	69%

Figure 1 TGF-β1 induces apoptosis in SNU-16 cells. SNU-16 cells were treated with 5 ng/ml of TGF-β1 for the indicated time periods and cells were collected for analysis. (**a**) the progression of cell cycle in TGF-β1-treated cells. At the indicated times of TGF-β1 treatment, cells were fixed with 70% ethanol, stained with propidium iodide, and subjected to flow cytometric analysis. The percentages of G1, S, G2/M, and sub-G1 phase cells were determined based on the DNA content histograms. (**b**) the induction of chromosomal DNA fragmentation by TGF-β1. Chromosomal DNAs were extracted from cells treated with TGF-β1 for the indicated times and electrophoresed in 1.5% agarose gel, as described in Materials and methods. DNA size marker (M) was used for running control. (**c**) the externalization of phosphatidylserine during TGF-β1-induced apoptosis. Annexin V staining combined with PI staining were performed in control cells or cells treated with TGF-β1 for 24 h and then analysed by flow cytometry. The percentage of cells in each window was indicated. The percentage of cells in the lower right quadrant dramatically increased in TGF-β1-treated cells

after stimulation in a time-dependent manner (Figure 3a). The p19 fragment was maximal at 24 h and declined thereafter (Figure 3a). This result was in accordance with a previous report that the active p17 fragment was derived from the p19 fragment (Martin *et al*., 1996). To verify that caspase-3 activity is well correlated with the appearance of the p17 fragment, we then examined whether poly (ADP-ribrose) polymerase (PARP) is cleaved in SNU-16 cells treated with TGF-β1. Native PARP (116 kDa) was cleaved into a typical apoptotic fragment of 85 kDa in TGF-β1-treated SNU-16 cells, and the kinetics of this cleavage were found to correlate with the kinetics of the appearance of the active p17 fragment of caspase-3 (Figure 3b). These results suggest that caspase-3 activation is involved in the TGF-β1-induced apoptosis of SNU-16 cells.

To assess the role of caspase-3 in the TGF-β1-induced apoptosis of SNU-16 cells, we next examined the effect of the specific caspase-3 inhibitor, Asp-Glu-Val-Asp-fluoromethylketone (DEVD-fmk), on both the apoptotic status and cell cycle distribution of TGF-β1-treated cells. After 36 h incubation with or without TGF-β1 in the absence or presence of 50 μM DEVD-fmk, cells were analysed by flow cytometry following PI staining of the cellular DNA. Single treatment with DEVD-fmk neither affected cell cycle distribution nor did it trigger cell death (Figure 4a,b). When TGF-β1 was treated alone, apoptotic cell death was induced up to 72% (7% in control cells) (Figure 4c). However, in the presence of DEVD-fmk, apoptosis was completely inhibited (3%) and, interestingly, most cells were arrested at the G1 phase of the cell cycle (89% *vs* 41% in control cells) (Figure 4d). A similar pattern was also observed with a broad range of caspases inhibitor, z-Val-Ala-Asp-fluoromethylketone (zVAD-fmk), at the same concentration (data not shown). These results indicate that TGF-β1-induced apoptosis is dependent on the activation of caspase-3 and that TGF-β1-mediated growth arrest is induced irrespective of caspase-3 activation in SNU-16 cells.

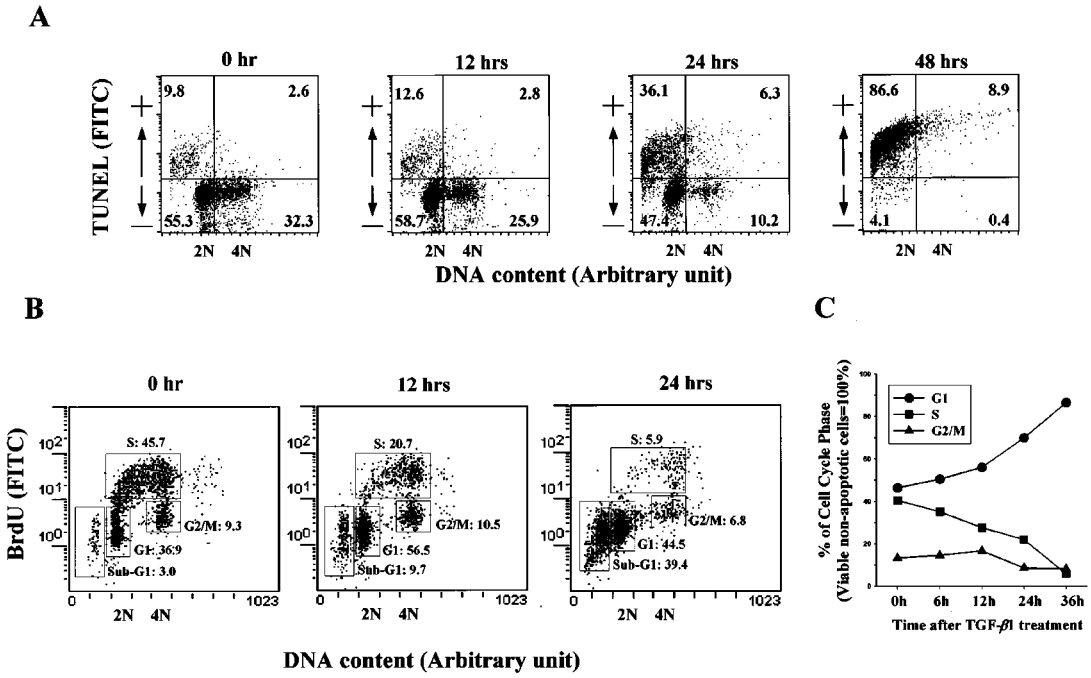

Figure 2 TGF-β1 induces initial G1 cell cycle arrest and subsequent G1 phas-specific apoptosis. (**a**). At the indicated time points, mock-treated (controls) or cells treated with 5 ng/ml of TGF-β1 were TUNEL-stained with FITC-labeled dUTP as described in Materials and methods and then stained with propidium iodide. Cells stained with both fluorescent dyes were analysed by flow cytometry. Three separate experiments gave similar results. TUNEL-positive (+) and TUNEL-negative (−) cells were divided by the horizontal line, and the G1 phase (2N) and S/G2/M phase (>2 N) were separated by the vertical line. (**b**) BrdU pulse labeling. At the indicated time points, cells were labeled with BrdU for 1 h and subjected to flow cytometry analysis as described in Materials and methods. The cell cycle positions were determined by analysing the correlated expression of total DNA content (abscissa) and incorporated BrdU levels (ordinate). The percentage of each region was indicated. (**c**) The percentage of each cell cycle phase was determined based on the DNA content in Figure 1a only with viable non-apoptotic cells (⩾2 N DNA contents)

Aberrant Cdk2 activation is involved in TGF-β1-induced Apoptosis

To determine whether the cell cycle machinery plays a role in the TGF-β1-induced apoptosis of SNU-16 cells, we analysed the activity of several Cdks in these cells. Since TGF-β1 induces G1 phase-specific apoptotic cell death in SNU-16 cells, the changes of G1 phase-related Cdks (Cdk2, Cdk4, and Cdk6) activities were checked during apoptosis. As shown in Figure 5a, Cdk2 kinase activity declined initially at 12 h after stimulation with TGF-β1, which suggests TGF-β1-mediated growth arrest. However, surprisingly, the Cdk2 kinase activity then aberrantly increased in a time-dependent manner. Moreover, the time course of Cdk2 activation was closely correlated with both a dramatic induction of apoptosis by TGF-β1 (Figures 1a and 5a) and caspase-3 activation (Figures 3a and 5a). However, aberrant activation of Cdk4 and Cdk6 kinases was not observed during TGF-β1-induced apoptosis (Figure 5b). After TGF-β1 treatment, Cdk4 kinase activity and its protein level remained unchanged and Cdk6 kinase activity and its protein level decline time-dependently. Since Cdk6 kinase drives cell cycle progression in the G1 phase by phosphorylating target proteins such as Rb, down-regulation of Cdk6 kinase may be involved in TGF-β1-induced growth arrest of SNU-16 cells. This is also supported by the previous report suggesting that down-regulations of Cdk6 protein and Cdk2 kinase activity are involved in TGF-β1-induced growth inhibition of mink lung epithelial cells (Tsubari *et al*., 1999). Thus, these results indicate that among the G1 phase-related Cdks, only Cdk2 kinase is abnormally activated during the TGF-β1-induced apoptosis of SNU-16 cells.

Inhibition of Cdk2 activity blocks TGF-β1-induced appoptosis of SNU-16 cells

To test whether aberrantly elevated Cdk2 activity is necessary for TGF-β1-induced apoptosis of SNU-16 cells, we examined the effect of roscovitine and olomoucine, specific inhibitors for both Cdk2 and Cdc2, on TGF-β1-induced apoptosis. Accordingly, SNU-16 cells were pretreated with roscovitine or olomoucine at various concentrations for 1 h, and then incubated with TGF-β1 for 36 h. Although a single treatment with roscovitine induced apoptotic cell death dose-dependently in SNU-16 cells, when cells so treated were challenged with TGF-β1, apoptosis was blocked in a dose-dependent manner (Figure 6a). In particular, cells treated with 20 μM of roscovitine prior to TGF-β1 treatment were almost resistant to TGF-β1-induced apoptosis, because the extent of apoptosis was similar to that of a roscovitine single treatment without the additional increase of apoptosis by TGF-β1 (Figure 6a). Cdk2 kinase activity was also inhibited dose-

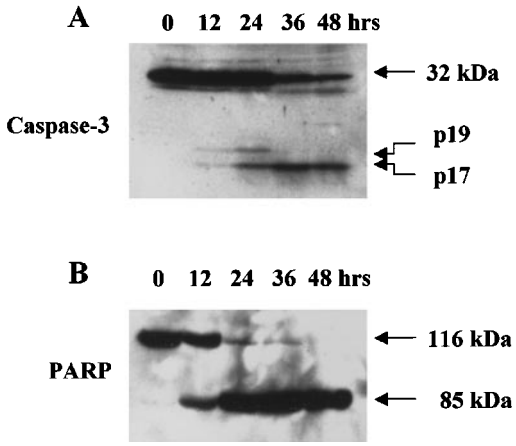

Figure 3 TGF-β1-induced apoptosis is associated with the activation of caspase-3. SNU-16 cells were treated with 5 ng/ml of TGF-β1 for the indicated times. (**a**) Equal amounts of cell extracts (100 μg) were resolved by SDS–PAGE and analysed by Western blotting with antibody specific for caspase-3. The proform (32 kDa) of caspase-3 and the p19 and p17 forms of cleaved caspase-3 were indicated. (**b**) Western blot analysis of PARP was performed as in (**a**) with antibody specific for PARP. Native PARP (116 kDa) and cleaved PARP (85 kDa) were indicated

dependently and almost suppressed at a concentration of 20 μM of roscovitine in the presence of TGF-β1 (eightfold decrease) (Figure 6b). Most significantly, the death-blocking effect of roscovitine closely correlated with the suppression of Cdk2 kinase activity considering that roscovitine alone also induced apoptosis (Figure 6a,b). To eliminate the possibility that roscovitine inhibits other G1 phase-related Cdks, we checked the effect of 20 μM of roscovitine on Cdk4 and Cdk6 kinases. As shown in Figure 6c, roscovitine dose not affect the activity of Cdk4 and Cdk6 kinases at 20 μM. Since roscovitine can also inhibit Cdc2 kinase activity, this was examined separately. However, Cdc2 kinase activity did not show any significant change during TGF-β1-induced apoptosis (data not shown). A similar result was obtained with olomoucine treatment, but at a higher concentration than that of roscovitine (Figure 6d and data not shown). Therefore, these results indicate that aberrantly elevated Cdk2 activity is required for the TGF-β1-induced apoptosis of SNU-16 cells.

Cdk2 activation during apoptosis results from caspase-3-mediated cleavage of p21 and p27

Biochemically, Cdk2 activity may be influenced by a change in its protein level, phosphorylation status, or its cyclin partners, cyclin E and A. In this study, the amount of Cdk2, cyclin E and A proteins were not changed during TGF-β1-induced apoptosis (Figures 5a: lower panel, and 7a). In addition, the relative abundance of the two Cdk2 bands detected by the anti-Cdk2 antibody did not change during apoptosis suggesting that the phosphorylation status of Cdk2 did not change and did not contribute to its effect on apoptosis (Figure 5a: lower panel).

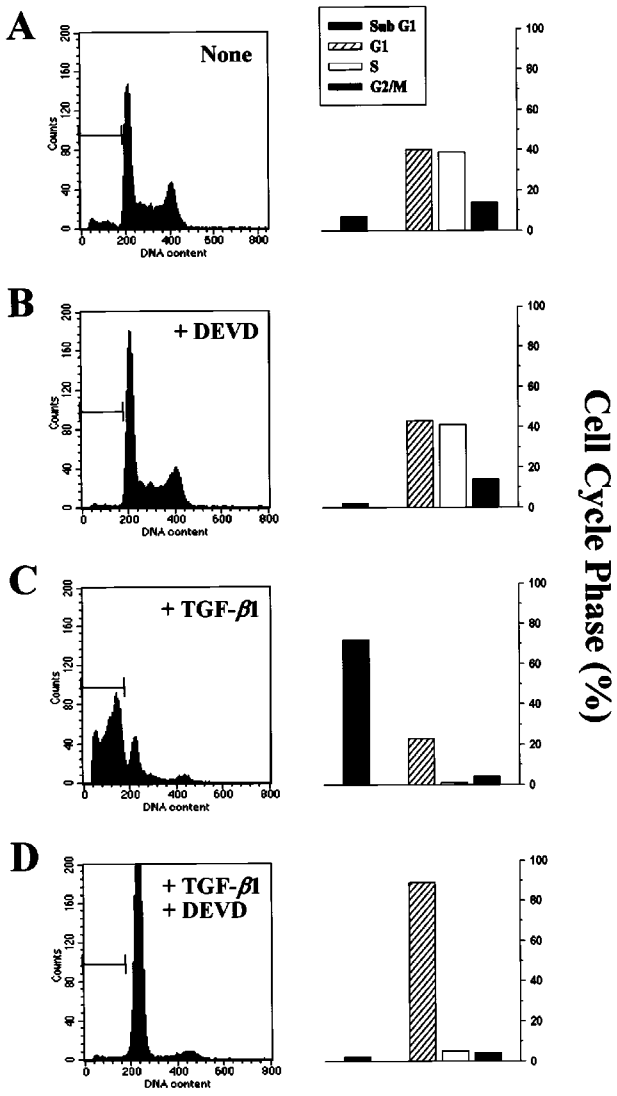

Figure 4 TGF-β1-induced apoptosis is dependent on but TGF-β1-induced G1 arrest is independent on caspase-3 activation. SNU-16 cells were incubated for 36 h with or without 5 ng/ml of TGF-β1 in the absence or the presence of 50 μM of DEVD-fmk. Each of the treatment groups, mock-treated (controls) (**a**), DEVD-fmk-treated (50 μM) (**b**), TGF-β1-treated (5 ng/ml) (**c**), and TGF-β1-treated cells in the presence of DEVD-fmk (**d**), was then analysed by flow cytometry after propidium iodide staining. The percentages of G1, S, G2/M, and sub-G1 cells (right panels) present were determined based on their DNA content histograms (left panels). Representative data from three independent experiments is shown

To understand the mechanism of aberrant Cdk2 activation in apoptotic cells, we next examined two Cdk inhibitors, p21 and p27, which are known to play major roles in the regulation of Cdk2 activity (Hunter and Pines, 1994; Sherr and Roberts, 1999), using Western blot analysis. Upon TGF-β1 treatment, the level of p21 was strongly induced for up to 24 h, which is another sign of initial G1 cell cycle arrest, and dramatically decreased thereafter. At the same time, we detected a 14 kDa fragment, which was maximal at

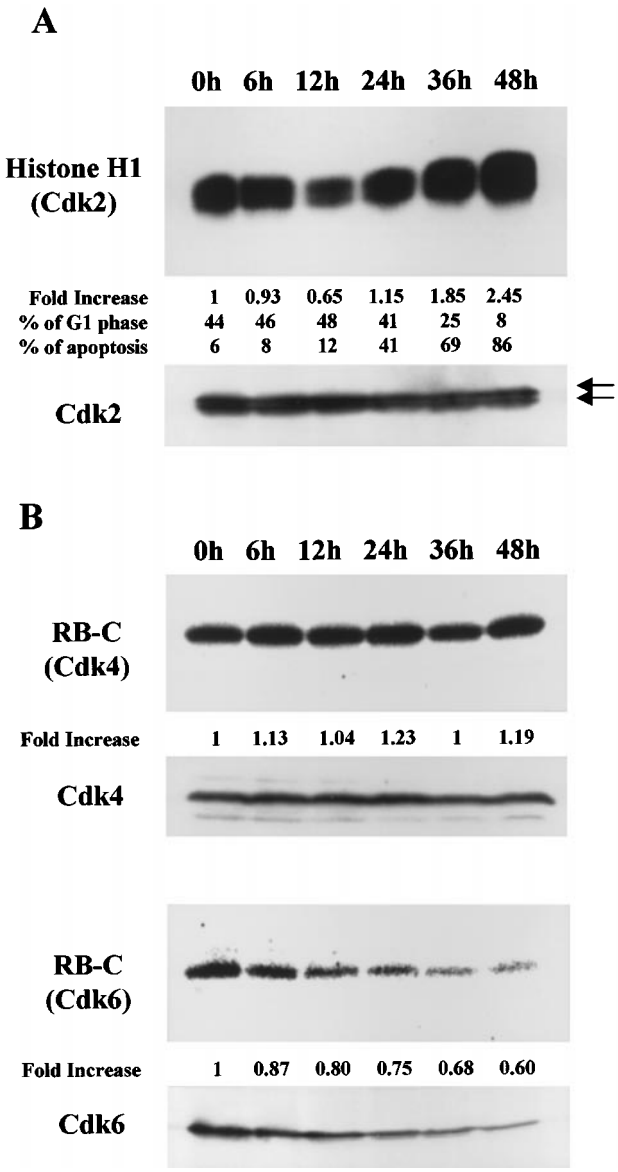

Figure 5 Aberrant activation of Cdk2 kinase is involved in TGF-β1-induced apoptosis (**a**) Cdk2 kinase activity. Whole cell extracts were prepared from SNU-16 cells treated with TGF-β1 for the indicated times and equal amounts of the extract (200 μg) were immunoprecipitated with anti-Cdk2. Anti-Cdk2 immune complex was used for the Cdk2 kinase assay, which was carried out using histone H1 as a substrate. Samples were analysed by SDS–PAGE and autoradiography. The data shown is representative of four independent experiments. Fold changes in Cdk2 kinase activity were determined by liquid scintillation counting of each gel slice and indicated as numbers. The level of Cdk2 protein was determined by Western blot analysis and two Cdk2 bands were indicated (lower panel). (**b**) Cdk4 and Cdk6 kinase activities. Anti-Cdk4 and anti-Cdk6 immune complexes were prepared as described in (**a**) and Cdk4 and Cdk6 kinase assays were performed using RB-C terminus fusion protein containing residues 769–921 as a substrate. One representative result of three independent experiments is shown. Fold changes in the respective kinase activities were calculated as described in (**a**). The changes of Cdk4 and Cdk6 protein level were determined by Western blot analyses and presented in each lower panel

24 h and then reduced in a time-dependent manner (Figure 7b). In the case of p27, the intact protein level was sustained for 12 h and then slowly decreased. In addition, we noted a faster migrating smaller fragment after 12 h and the status of this fragment slightly increased thereafter (Figure 7b). Recently, several reports have demonstrated that p21 and p27 could be cleaved by caspase-3 during apoptosis induced by a variety of stimuli (Levkau *et al*., 1998; Zhou *et al*., 1998; Zhang *et al*., 1999). Since Western blot analyses of p21 and p27 were performed with their specific monoclonal antibodies, our results demonstrated that two Cdk inhibitors from TGF-β1-treated cells generated additional truncated fragments. Of note, we found that the change in Cdk2 kinase activity was closely connected with the truncations of p21 and p27 (Figures 5a and 7b). To show the direct link between the levels of Cdk inhibitors and the changes of Cdk2 kinase activity in control or TGF-β1-treated cells, we immunoprecipitated Cdk2 from control or TGF-β1-treated cell lysates, respectively and then determined the levels of p21 and p27 associated with Cdk2. As shown in Figure 7c, the level of p21 associated with Cdk2 significantly increased at 12 h, which explains the initial down-regulation of Cdk2 kinase activity for G1 cell cycle arrest (Figure 5a), and then dramatically decreased at 48 h. We could not detect the fragment of p21 in Cdk2 immunoprecipitates. In the case of p27, the intact protein level associated with Cdk2 slightly increased at 12 h and strongly declined at 48 h. In addition, the fragment of p27 associated with Cdk2 was detected at 48 h, but its level was dramatically lower than that of intact p27 in control cells (Figure 7c), which has been also observed in the previous report (Levkau *et al*., 1998). Therefore, these results suggest that the truncations and loss of both Cdk inhibitors contribute to aberrant Cdk2 activation during TGF-β1-induced apoptosis..

To assess whether proteolytic cleavage by caspase-3 is responsible for the truncations of these Cdk inhibitors during apoptosis, we investigated the effects of cell permeable caspase-3 inhibitor, DVED-fmk, on the protein cleavage. As shown in Figure 7d, pretreatment with 50 μM of DEVD-fmk completely prevented the production of the truncated forms of p21 and p27. These results show that caspase-3 is responsible for the proteolytic cleavage of p21 and p27 in TGF-β1-induced apoptosis. Moreover, p21 was left in the induced state and p27 was maintained at non-treated cell levels in the presence of DEVD-fmk (Figure 7d), suggesting that the treatment with DEVD-fmk may inhibit aberrant activation of Cdk2 through preventing caspase-3-mediated cleavage of both Cdk inhibitors. To confirm this, we investigated the change of Cdk2 kinase activity in the presence of DEVD-fmk. As shown in Figure 7e, Cdk2 kinase activity decreased time-dependently without aberrant activation, which is also well matched to the result that most TGF-β1-treated cells are arrested at the G1 phase without the induction of apoptosis in the presence of DEVD-fmk (Figure 4d). Thus, our results suggest that the cleavage and loss of p21 and p27 by caspase-3 contribute to not only aberrant Cdk2 activation, but also to the

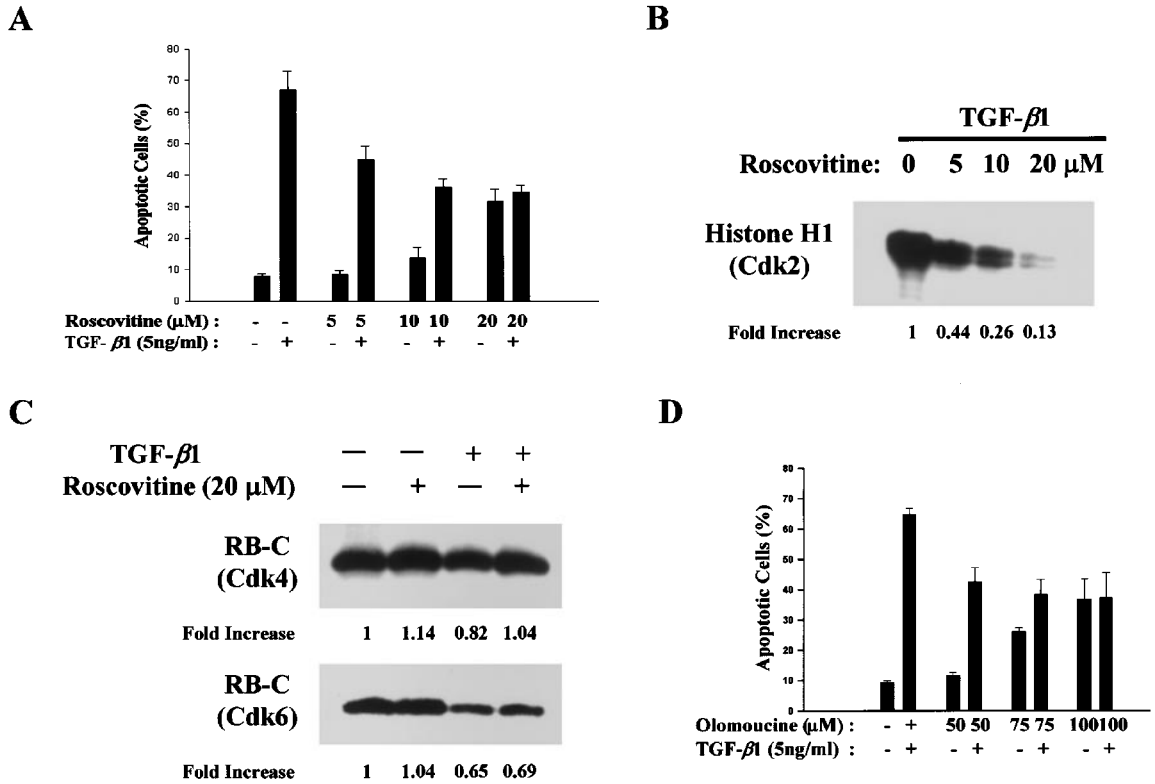

Figure 6 Roscovitine and olomoucine, both potent inhibitors of Cdk2 kinase, efficiently block TGF-β1-induced apoptosis. (**a**) SNU-16 cells were pretreated with roscovitine at the indicated concentrations for 1 h and then incubated with (+) or without (−) TGF-β1 (5 ng/ml) for 36 h. The induction of apoptosis was measured by propidium iodide staining followed by flow cytometry. Cells with less than 2 N of DNA content were counted as apoptotic cells and the percentages of apoptotic cells were illustrated graphically. Data is presented as mean ± s.d. of three separate experiments of duplicate determinations. (**b**) Cells were pretreated with roscovitine at the indicated concentrations for 1 h and then incubated with TGF-β1 (5 ng/ml) for 36 h. Cell lysates were prepared and Cdk2 kinase assay was carried out as described in Figure 5a. (**c**) Cell extracts were prepared from SNU-16 cells stimulated with (+) or without (−) TGF-β1 (5 ng/ml) for 36 h in the presence (+) or absence (−) of 20 μM of roscovitine and subjected to Cdk4 and Cdk6 kinase assay as described in Figure 5b. (**d**) Cells were pretreated with olomoucine at the indicated concentrations for 1 h and then incubated with (+) or without (−) TGF-β1 (5 ng/ml) for 36 h. Data is presented as described in (**a**)

disruption of TGF-β1-mediated G1 cell cycle arrest that in turn renders SNU-16 cells more sensitive to G1 phase-specific apoptosis.

Cdk2 acts downstream of caspase-3 activation as an essential effector in TGF-β1-induced apoptosis

We observed that inhibitors of caspase-3 and Cdk2 efficiently blocked TGF-β1-induced apoptosis respectively (Figures 4d and 6a,d) and also found that the activation of caspase-3 precedes the activation of Cdk2 in TGF-β1-induced apoptosis (Figure 7e). To determine which activity between of caspase-3 and Cdk2 is essential for TGF-β1-induced apoptosis, we examined whether caspase-3 activation and the subsequent cleavage of p21 and p27 still occur even when TGF-β1-induced apoptosis is blocked by the suppression of Cdk2 activity. To test this, Western blot analyses of caspase-3, p21, and p27 were performed with apoptosis-inhibited SNU-16 cells by pretreatment with 20 μM of roscovitine. As shown in Figure 8, a single treatment with TGF-β1 for 24 h induced caspase-3 activation and subsequent cleavage of all tested proteins, whereas roscovitine alone did not. When roscovitine was treated together with TGF-β1, all tested proteins exhibited additional cleaved forms, similar to that of TGF-β1 alone (Figure 8). These results indicate that activated Cdk2 as a downstream effector of activated caspase-3 plays an essential role in TGF-β1-induced apoptosis, and that caspase-3 activation and subsequent cleavage of p21 and p27, while necessary, are not sufficient for TGF-β1-induced apoptosis. Thus, it is likely that a requisite function of caspase-3 for TGF-β1-induced apoptosis is the activation of effector Cdk2 through the truncation of p21 and p27 in SNU-16 cells.

Rb is another target of caspase-3 but the cleavage of Rb play minor roles in TGF-β1-induced apoptosis of SNU-16 cells

Two recent reports have suggested that Rb is a possible major target for the induction of apoptosis by TGF-β1 (Schrantz *et al*., 1999; Choi *et al*., 1999). Choi *et al*. (1999) reported that transiently activated Cdc2 and

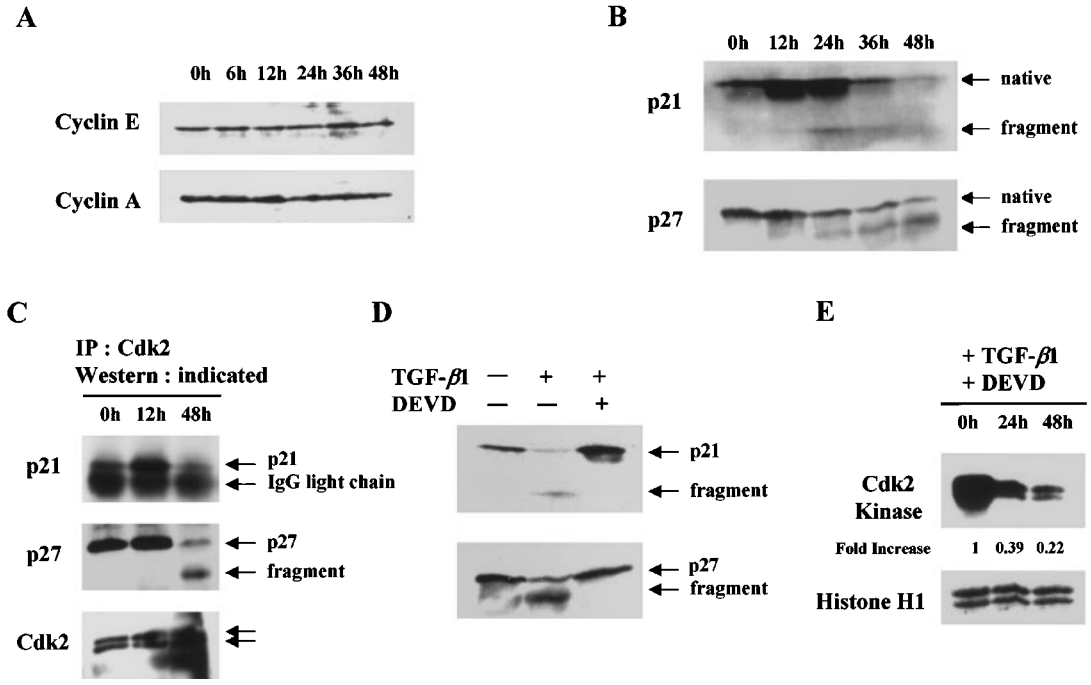

Figure 7 Aberrant Cdk2 activation is caused by caspase-3-mediated cleavage of $p21^{waf1}$ and $p27^{kip1}$. SNU-16 cell extracts were prepared from the respective cells treated with 5 ng/ml of TGF-β1 for the indicated time periods. Western blot analyses were then performed with antibodies specific to cyclin E and A (**a**), and with monoclonal antibodies specific to p21 and p27 (**b**). (**c**) Cdk2 was immunoprecipitated (IP) from the control cells and cells treated with TGF-β1 for 12 and 48 h, and then p21 and p27 associated with Cdk2 were evaluated by Western blot analyses. Amount of immunoprecipitated kinases were determined by incubating blots with anti-Cdk2 antibody. (**d**) Cells were incubated for 48 h with (+) or without (−) 5 ng/ml of TGF-β1 in the presence (+) or absence (−) of 50 μM of DEVD-fmk. Whole cell extracts were prepared from each of the treatment groups and Western blot analyses were then performed as described in Materials and methods. (**e**) Cell extracts were prepared from TGF-β1-treated cells for the indicated time periods in the presence of DEVD-fmk (50 μM) and subjected to Cdk2 kinase assay as described in Figure 5a

Cdk2 by TGF-β1 trigger apoptosis through the hyperphosphorylation of Rb in FaO rat hepatoma cells. Meanwhile, Schrantz *et al.* (1999) reported that TGF-β1-induced apoptosis of human B lymphocytes is dependent on caspase activation and caspase-dependent cleavage of Rb. To check these possibilities in our systems, we examined the status of Rb during the TGF-β1-induced apoptosis of SNU-16 cells. Western blot analysis with a specific monoclonal antibody to Rb showed that, without any sign of hyperphosphorylation of Rb, the hypophosphorylated forms of Rb, which associated with cell growth arrest, accumulated and the total amount of native Rb declined in a time-dependent manner (Figure 9a). Simultaneously, the additional truncated form of Rb appeared (Figure 9a). Pretreatment with 50 μM DVED-fmk completely abolished the truncated form of Rb, and Rb accumulated in its hypophosphorylated forms (Figure 9b). These results indicate that Rb is another target of caspase-3 during TGF-β1-induced apoptosis.

Our results showed that Cdk2 activation is critical for TGF-β1-induced apoptosis in SNU-16 cells. The link between Rb and Cdk2 activation has been previously explained on the basis that inactivation of Rb is involved in the induction of cyclin E and A through E2F release, which in turn regulates Cdk2 activation to enforce Rb phosphorylation as a positive feedback loop (Girard *et al.*, 1991; Ohtsubo *et al.*, 1995). In our systems, caspase-3-mediated cleavage and loss of Rb showed no effects on the induction of cyclin E or A during apoptosis (Figure 7a). Moreover, the caspase-3-mediated cleavage of Rb still occur even when TGF-β1-induced apoptosis is blocked by the inhibition of Cdk2 (Figure 9c), which suggests that the cleavage of Rb is not directly involved in the Cdk2 activation and induction of apoptosis by TGF-β1 in SNU-16 cells. Alternatively, as the activity of Rb has been shown to be required for TGF-β1 to efficiently suppress cell growth (Laiho *et al.*, 1990; Pietenpol *et al.*, 1990), it is likely that caspase-mediated cleavage and loss of Rb may contribute to the disruption of G1 cell cycle arrest by TGF-β1, which make cells more sensitive to G1 phase specific apoptosis.

Discussion

Although TGF-β1 has been implicated in apoptosis induction in a variety of cell types, the underlying molecular mechanism by which TGF-β1 induces apoptosis remains largely undefined. In particular, the relationship between the signaling pathways leading to TGF-β1-induced apoptosis and TGF-β1-mediated cell cycle arrest are almost unexplored. In

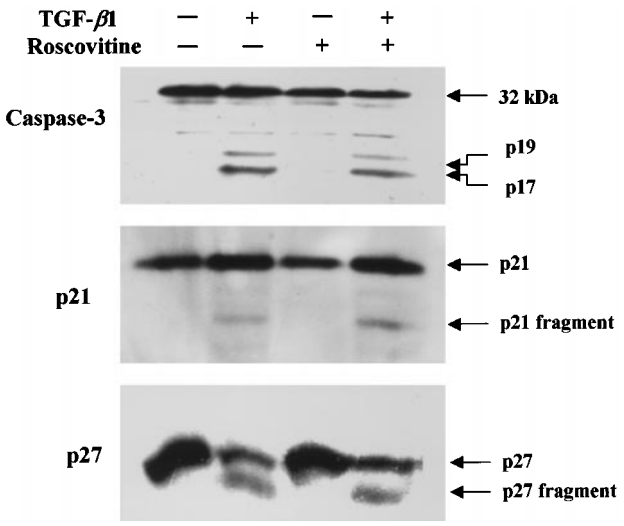

Figure 8 Cdk2 acts downstream of caspase-3 as an essential effector in the TGF-β1-induced apoptosis of SNU-16 cells. Cell extracts were prepared from SNU-16 cells stimulated with (+) or without (−) TGF-β1 (5 ng/ml) for 24 h in the presence (+) or absence (−) of 20 μM of roscovitine. Equal amounts of cell extracts were resolved by SDS–PAGE and analysed by Western blotting with antibodies specific for the indicated proteins. Truncated forms of indicated proteins were generated in both apoptosis-induced cells by TGF-β1 and apoptosis-inhibited cells by roscovitine

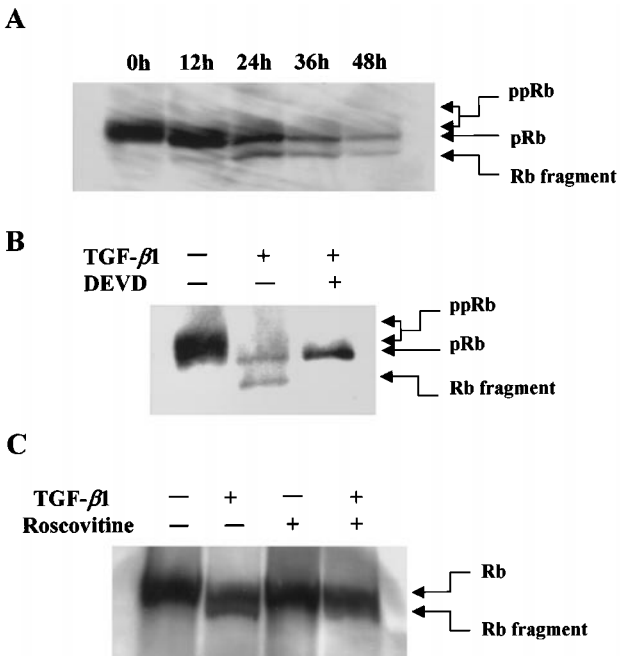

Figure 9 Rb is another target of caspase-3. (**a**) Whole cell extracts were prepared from the respective cells treated with TGF-β1 (5 ng/ml) for the indicated time periods. Western blot analysis was then performed with monoclonal antibody specific for Rb. Hyperphosphorylated forms of Rb (ppRb), hypophosphorylated forms of Rb (pRb), and Rb fragment were indicated. (**b**) Cells were incubated for 48 h with (+) or without (−) TGF-β1 (5 ng/ml) in the presence (+) or absence (−) of DEVD-fmk (50 μM). Whole cell extracts were then prepared from each of the treatment groups and Western blot analyses performed as described in (**a**). (**c**) Cell extracts were prepared from SNU-16 cells stimulated with (+) or without (−) TGF-β1 (5 ng/ml) for 24 h in the presence (+) or absence (−) of 20 μM of roscovitine and then analysed by Western blotting as described in (**a**)

this study, we found that TGF-β1-mediated G1 cell cycle arrest is constantly induced in SNU-16 cells irrespective of caspase-3 activation. However, activated caspase-3 leads to the cleavage and loss of native p21, p27, and Rb proteins, contributing to the disruption of TGF-β1-mediated growth arrest. Subsequently, activated Cdk2 resulting from the cleavage of Cdk inhibitors drives TGF-β1-treated cells into apoptotic cell death. Cumulatively, these findings suggest a new molecular mechanism for TGF-β1-induced apoptosis, in particular, that TGF-β1 induces growth arrest and then drives such cells to apoptosis.

Although the phenomenon of both TGF-β1-induced growth arrest and TGF-β1-induced apoptosis in the same cells has been observed previously, the explanation for this has not been provided. In the present study, we found that caspase-3 activity is involved in the disruption of TGF-β1-mediated G1 arrest in SNU-16 cells. Our results showed that p21, p27, and Rb, which are clearly involved in TGF-β1-induced G1 cell cycle arrest, are all cleaved by caspase-3 and their levels decrease during TGF-β1-induced apoptosis (Figures 7d and 9b). Indeed, all these proteins have been shown to contain a consensus caspase-3 cleavage site at the C termini (Levkau *et al*., 1998; Tan and Wang, 1998). We also observed that, in the presence of caspase-3 inhibitor, most TGF-β1-treated cells were arrested at the G1 phase without the induction of apoptosis (Figure 4d). In addition, only hypophosphorylated forms of Rb accumulated (Figure 9b) and Cdk2 kinase activity continuously decreased because both p21 and p27 remained in the intact state (Figure 7d,e), which are also indicative of TGF-β1-induced G1 arrest. Thus, based on our present results, we propose that caspase-3 triggers the disruption of TGF-β1-mediated growth arrest through the cleavage of p21, p27, and Rb, which in turn make cells sensitive to G1 phase-specific apoptotic cell death.

Recent studies have suggested that apoptosis is closely linked to aberrations in the activity of cyclin-dependent kinases, including Cdk2. Evidence for the essential role of Cdk2 in apoptosis is provided by the observation that PC12 cells are protected from growth factor deprivation-induced apoptosis by pharmacological Cdk2 inhibitors (Park *et al*., 1996), and that TNFα- staurosporine- and serum deprivation-induced apoptosis are blocked by dominant-negative Cdk2 (Meikrantz and Schlegel, 1996; Levkau *et al*., 1998; Harvey *et al*., 2000), and that the overexpression of wild-type Cdk2 accelerates thymocyte apoptosis (Gil-Gómez *et al*., 1998). In this study, we observed that Cdk2 kinase was aberrantly

activated after 24 h of TGF-β1 treatment (Figure 5a), without the activation of other G1 phase-related Cdks (Figure 5b). The significance of Cdk2 activation in TGF-β1-induced apoptosis of SNU-16 cells was demonstrated by the fact that pretreatment with roscovitine or olomoucine, both potent Cdk2 inhibitors, efficiently blocked TGF-β1-induced apoptosis (Figure 6a,d). In particular, direct correlation was observed between Cdk2 activation and the dramatic induction of apoptosis in response to TGF-β1 (Figures 1a and 5a). These results indicate that Cdk2 activation is necessary for the TGF-β1-induced apoptosis of SNU-16 cells. However, the specific targets of Cdk2 activity with respect to the effector phase of TGF-β1-induced apoptotic pathway need to be investigated further.

In SNU-16 cells, a single treatment with roscovitine triggered apoptotic cell death dose-dependently. Indeed, it was recently reported that roscovitine could induce apoptotic cell death in breast cancer cells (Mgbonyebi *et al*., 1999). If roscovitine could not affect TGF-β1-induced apoptosis in our sytems, the extent of apoptosis in cells treated with both roscovitine and TGF-β1 should be much higher than that of a single treatment due to the additive effect. However, since the lower and similar extent of apoptosis were observed in cells treated with both TGF-β1 and roscovitine (Figure 6a), the death-blocking effect of roscovitine is clear in our systems. In this regard, the suppression of Cdk2 activity by roscovitine is closely correlated with the inhibition of TGF-β1-induced apoptosis considering that roscovitine itself also induced apoptosis (Figure 6a,b). In particular, roscovitine treatment did not induce caspase-3 activation and subsequent cleavage of p21, p27, and Rb (Figures 8 and 9c), which indicated that the intracellular events of TGF-β1-induced apoptosis are clearly different from those of roscovitine-induced apoptosis.

Our studies suggest that the activation of Cdk2 is caused by caspase-3-dependent cleavage of p21 and p27. The protein level or phosphorylation status of Cdk2 kinase did not change, moreover, its cyclin partners, cyclin E and cyclin A, also showed no significant changes (Figures 5a and 7a). In addition, the reduction of native p21 and p27 proteins by caspase-mediated cleavage correlated well with the activation of Cdk2 kinase (Figures 5a and 7b). Most of all, the direct association between both Cdk2 inhibitors and Cdk2 dramatically decreased during TGF-β1-induced apoptosis (Figure 7c). In particular, in our systems, it seems that p21 is more directly involved in regulating Cdk2 activation, because the status of p21 and its association with Cdk2, that initially increased and later reduced, coincide well with the change in Cdk2 activity that is initially decreased and later increased. A similar explanation for the mechanism of caspase-mediated Cdk2 activation was provided by a previous report, which stated that the cleavage of p21 and p27 at the C terminus, containing nuclear localization signal, altered their intracellular localizations from nucleus to cytoplasm and resulted in Cdk2 activation through their loss from Cdk2/cyclins complex in serum deprivation-induced apoptosis (Levkau *et al*., 1998).

The most interesting finding during the course of this study was that the actual function of caspase-3 for the TGF-β1-induced apoptosis of SNU-16 cells was not the cleavage event itself but the activation of Cdk2 as a downstream effector through the breakdown of p21 and p27. These results agree well with a recent report, which suggested that caspase activity alone is insufficient for the full physiological cell death program and that caspase-dependent Cdk activity is requisite for apoptotic cell death (Harvey *et al*., 2000). However, there is also a distinct report, which suggested that Cdk2 functions upstream of caspase activation and caspase-dependant proteolytic cleavage in thymocyte apoptosis (Hakem *et al*., 1999). In our systems, the cleavage of p21, p27, and Rb by caspase-3 was still observed even when TGF-β1-induced apoptosis was blocked by the suppression of Cdk2 activity (Figures 8 and 9c). Thus, in SNU-16 cells, Cdk2 activity may be the essential effector of TGF-β1-induced apoptosis acting downstream of the caspase-dependent cleavage of p21, p27, and Rb.

Recently, several reports have suggested that the caspase-mediated cleavage of Rb or p21 is critical for the induction of apoptosis (Schrantz *et al*., 1999, Tan and Wang, 1998; Zhang *et al*., 1999). They stressed the protective roles of Rb and p21 against apoptosis (Howes *et al*., 1994; Wang and Walsh, 1996), based on the observation that the overexpression of cleavage-resistant Rb or p21 mutant efficiently suppressed apoptosis induced by a variety of stimuli. However, they did not extend their studies to the examination of the involvement of Cdk kinases. In our experimental systems, caspase-mediated cleavage of Rb and p21, which are known to be general protective factors against apoptosis (Howes *et al*., 1994.; Wang and Walsh, 1996), were identified as upstream events of Cdk2 activation, implying that the previous results about the effect of uncleavable Rb and p21 can also be explained by our present results. In addition, the blockade of Cdk2 activation still inhibited apoptosis even when protective factors such as Rb and p21 were cleaved. Therefore, in SNU-16 cells, it is evident that catastrophic Cdk2 activity resulting from caspase-mediated cleavage of Cdk inhibitors is the actual effector of TGF-β1-induced apoptosis.

In conclusion, we suggest a new molecular mechanism for TGF-β1-induced apoptosis in SNU-16 cells as follows. TGF-β1 induces the initial G1 cell cycle arrest and also triggers caspase-3 activation in SNU-16 cells. Caspase-mediated cleavage of p21, p27, and Rb then results in the disruption of cell cycle arrest and aberrant Cdk2 activation. Ultimately, this Cdk2 activation is the critical step, which leads the cells to irreversible apoptotic cell death.

Materials and methods

Reagents

Antibodies to Caspase3 (H-277), Cdk2 (M2), Cdk4 (H-22), Cdk6 (C-21), Cyclin E (C-19), and Cyclin A (BF683) were purchased from Santa Cruz Biotechnology, Inc. (Santa Cruz, CA, USA). Antibodies to p21 (C24420) and p27 (K25020) were obtained from Transduction Laboratories (Lesington, KY, USA). Antibodies to RB (G3-245) and PARP (7D3-6) were provided by PharMingen (San Diego, CA, USA). zVAD-fmk, DEVD-fmk, olomoucine, and roscovitine were purchased from Calbiochem-Novabiochem Corp. (San Diego, CA, USA). Histone H1 was obtained from Boehringer Mannheim (Germany) and recombinant RB-C terminus fusion protein containing residues 769–921 was purchased from Santa Cruz Biotechnology (Santa Cruz, CA, USA).

Cell culture

SNU-16 human gastric carcinoma cell line (purchased from Korea Cell Line Bank, Seoul, Korea) has been directly established from the malignant ascite of a gastric cancer patient (Park *et al*., 1994). Cells were cultured in RPMI-1640 medium supplemented with 10% fetal bovine serum in a humidified atmosphere of 5% CO_2 at 37°C. In all experiments, TGF-β1 (5 ng/ml) was treated on the day after seeding.

Chromosomal DNA isolation and ladder formation assay

Cells were harvested by centrifugation, and then suspended in a lysis buffer (50 mM Tris-Cl, pH 8.0, 10 mM EDTA, and 0.5% Laurylsarcosine) containing 50 μg/ml RNase A. After incubation at 37°C for 1 h, proteinase K was added to the cell lysate at a concentration of 50 mg/ml and samples were further incubated at 55°C for 4 h. Chromosomal DNA was purified by phenol/cloroform extraction and precipitated with ethanol. The quantity and the quality of the DNA obtained were determined spectrophotometrically. Ten micrograms of chromosomal DNA was electrophoresed in 1.5% agarose gel and visualized by ethidium bromide staining.

Cell cycle analysis

Cells were washed twice with PBS, and then fixed with 70% ethanol for 1 h. Fixed cells were washed with PBS, and stained with 50 μg/ml PI containing 50 μg/ml RNase A. The DNA content of cells (10 000 cells/experimental group) was analysed using a FACSCalibur flow cytometer (B&D, Mountain View, CA, USA) and a ModFit LT program (Verity Software House Inc.).

TUNEL and Annexin V analysis combined with PI staining

TUNEL was performed using an *in situ* cell death detection kit (Boehringer Mannheim, Germany) according to the manufacturer's recommendations. In brief, harvested cells were fixed in 4% paraformaldehyde at room temperature for 15 min, and permeabilized with 0.1% Triton X-100. Fixed cells were labeled with FITC-dUTP using terminal deoxythymidine transferase and stained with 5 μg/ml PI. DNA content and FITC labels of cells (10 000 cells/experimental group) were analysed using a FACSCalibur flow cytometer. To evaluate apoptotic cells, we also performed annexin V staining combined with PI staining because annexin V can detect the externalization of phosphatidylserine during the apoptotic progression. Annexin V staining was carried out using an annexin V assay kit (PharMingen, San Diego, CA, USA) according to the manufacturer's recommendations. In brief, prepared cells were washed twice with cold PBS and then resuspended in binding buffer (10 mM HEPES/NaOH, pH 7.4, 140 mM NaCl, 2.5 mM $CaCl_2$). Then, both 5 μl of annexin V-FITC (PharMingen, San Diego, CA, USA) and 10 μl of 20 μg/ml PI were added to these cells, which were later analysed with a FACSCalibur flow cytometry (B&D, Mountain View, CA, USA).

BrdU pulse labeling assay

Cells were labeled with BrdU for 1 h before harvesting and then fixed with 70% ethanol. Fixed cells were washed twice with PBS and then stained with a FITC-labeled anti-BrdU antibody (B&D, Mountain View, CA, USA) according to the manufacturer's protocol.

Western blot analysis

Cells were washed with PBS and then suspended in an extraction buffer (20 mM Tris-Cl, pH 7.4, 100 mM NaC1, 1% NP-40, 0.5% sodium deoxycholate, 5 mM $MgC1_2$, 0.1 mM PMSF, 0.1 mM pepstatin A, 0.1 mM antipain, 0.1 mM chymostatin, 0.2 mM leupeptin, 10 μg/ml aprotinin, 0.5 mg/ml soybean Trypsin inhibitor, and 1 mM benzamidine) on ice for 15 min. Lysates were cleared by centrifugation at 13 000 r.p.m. for 20 min. Equal amounts of cell extracts (100 μg) were resolved on SDS-polyacrylamide denaturing gels, transferred onto nitrocellulose membranes (Schleicher & Schuell, Germany), and probed with antibodies, as recommended by the manufacturer. Detection was performed using an ECL system (Amersham Pharmacia Biotech).

Immunoprecipitation and kinase assay

Cells were collected at intervals after TGF-β1 treatment and washed with PBS. They were then suspended in an extraction buffer (50 mM Tris-Cl, pH 7.5, 250 mM NaC1, 0.1% NP-40, 5 mM EDTA, 50 mM NaF, 0.1 mM $NaVO_4$, 100 mM PMSF, 0.2 mM leupeptin, 10 μg.ml aprotinin, 0.1 mM pepstatin A, and 0.1 mM antipain), and incubated on ice for 15 min. After centrifugation at 13 000 r.p.m. for 20 min, supernatant was collected as cell extract. Protein concentrations were determined using a Bio-Rad assay kit (Hercules, CA, USA). Two micrograms of each antibody (Cdk2, Cdk4, and Cdk6) were added to 200 μg of cell extracts in 500 μl of extraction buffer and incubated for 4 h at 4°C with continuous agitation. To collect immune complexes, 30 μl of protein A/G-agarose (Oncogene Research Products, Cambridge, MA, USA) was added to the mixture, which was then further incubated for 2 h. Immune complexes were centrifuged at 3000 r.p.m. for 5 min, precipitates were washed three times with extraction buffer and twice with kinase reaction buffer (50 mM Tris-Cl, pH 7.5, 10 mM $MgCl_2$, 1 mM DTT). Cdk2 kinase assays on histone H1 were performed by mixing the respective immune complexes with 5 μg of histone H1 and 10 μCi of [γ-^{32}P]ATP in 35 μl of kinase reaction buffer. Cdk4 and Cdk6 kinase assays on RB were carried out in the same way using 5 μg of recombinant RB-C terminus fusion protein (Santa Cruz Biotechnology, Santa Cruz, CA, USA). Kinase reactions were performed at 37°C for 30 min and then

terminated with 2× SDS–PAGE loading buffer. The reaction mixtures were resolved by SDS- polyacrylamide gel electrophoresis. Gels were stained with Coomassie Blue staining solution and dried. The extent of phosphorylation was measured by liquid scintillation counting of the gel slices of each substrate.

Acknowledgments
This work was supported by the Korean Ministry of Health and Welfare Grant HMP-99-M-03-0001 and by 1999 BK21 Project for Medicine. We are grateful to EK Kim for the flow cytometric analysis and TY Kim for manuscript preparation.

References

Alexandrow MG and Moses HL. (1995). *Cancer Res.,* **55,** 1452–1457.
Chen RH and Chang TY. (1997). *Cell Growth Differ.,* **8,** 821–827.
Choi KS, Eom YW, Kang Y, Ha MJ, Rhee H, Yoon J and Kim S. (1999), *J. Biol. Chem.,* **274,** 31775–31783.
Choi KS, Lim IK, Brady JN and Kim S. (1998). *Hepatology,* **27,** 415–421.
Datto MB, Li Y, Panus JF, Howe DJ, Xiong Y and Wang XF. (1995). *Proc. Natl. Acad. Sci. USA,* **92,** 5545–5549.
Ewen ME, Sluss HK, Whitehouse LL and Livingston DM. (1993). *Cell,* **74,** 1009–1020.
Faleiro L, Kobayashi R, Fearnhead H and Lazebnik Y. (1997). *EMBO J.,* **16,** 2271–2281.
Fan G, Ma X, Kren BT and Steer CJ. (1996). *Oncogene,* **12,** 1909–1919.
Fotedar R, Flatt J, Gupta S, Margolis RL, Fitzgerald P, Messier H and Fotedar A. (1995). *Mol. Cell. Biol.,* **15,** 932–942.
Geng Y and Weinberg RA. (1993). *Proc. Natl. Acad. Sci. USA,* **90,** 10315–10319.
Gil-Gómez G, Berns A and Brady HJ. (1998). *EMBO J.,* **17,** 7209–7218.
Girard F, Strausfeld U, Fernandez A and Lam NJC. (1991). *Cell,* **67,** 1169–1179.
Hakem A, Sasaki T, Kozieradzki I and Penninger JM. (1999). *J. Exp. Med.,* **189,** 957–967.
Hannon GJ and Beach D. (1994). *Nature,* **371,** 257–261.
Harvey KJ, Lukovic D and Ucker DS. (2000). *J. Cell. Biol.,* **148,** 59–72.
Howes KA, Ransom N, Papermaster DS, Lasudry JG, Albert DM and Windle JJ. (1994). *Genes Dev.,* **8,** 1300–1310.
Hunter T and Pines J. (1994). *Cell,* **79,** 573–582.
King KL and Cidlowski JA. (1995). *J. Cell. Biochem,* **58,** 175–180.
Kingsley DM. (1994). *Genes Dev.,* **8,** 133–146.
Ko TC, Sheng HM, Reisman D, Thompson EA and Beauchamp RD. (1995). *Oncogene,* **10,** 177–184.
Koff A, Ohtsuki M, Polyak K, Roberts JM and Massagué J. (1993). *Science,* **260,** 536–539.
Lafon C, Mathieu C, Guerrin M, Pierre O, Vidal S and Valette A. (1996). *Cell Growth & Differ.,* **7,** 1095–1104.
Laiho M, DeCaprio JA, Ludlow JW, Livingston DM and Massagué J. (1990). *Cell,* **62,** 175–185.
Levkau B, Koyama H, Raines EW, Clurman BE, Herren B, Orth K, Roberts JM and Ross R. (1998). *Mol. Cell.* **1,** 553–563.
Martin SJ, Amarante-Mendes GP, Shi L, Chuang TH, Casiano CA, O'Brien GA, Fitzgerald P, Tan EM, Bokoch GM, Greenberg AH and Green DR. (1996). *EMBO J.,* **15,** 2407–2416.
Meikrantz W and Schlegel R. (1995). *J. Cell. Biochem.,* **58,** 160–174.
Meikrantz W and Schlegel R. (1996). *J. Biol. Chem.,* **271,** 10205–10209.
Mgbonyebi OP, Russo J and Russo IH. (1999). *Cancer Res.,* **59,** 1903–1910.
Ohtsubo M, Theodoras AM, Schumacher J, Roberts JM and Pagano M. (1995). *Mol. Cell. Biol.,* **15,** 2612–2624.
Park DS, Farinelli SE and Greene LA. (1996). *J. Biol. Chem.,* **271,** 8161–8169.
Park JG, Frucht H, LaRocca RV, Bliss DPJ, Kurita Y, Chen T, Henslee JG, Trepel JB, Jensen RT, Johnson BE, Bang Y, Kim J and Gazdar AF. (1990). *Cancer Res.,* **50,** 2773–2780.
Park K, Kim S, Bang Y, Park J, Kim NK, Roberts AB and Sporn MB. (1994). *Proc. Natl. Acad.Sci. USA,* **91,** 8772–8776.
Patel T, Gores GJ and Kaufmann SH. (1996). *FASEB J.,* **10,** 587–597.
Pietenpol JA, Stein RW, Moran E, Yaciuk P, Schlegel R, Lyons RM, Pittelkow MR, Munger K, Howley PM and Moses HL. (1990). *Cell,* **61,** 777–785.
Polyak K, Kato JY, Solomon MJ, Sherr CJ, Massagué J, Roberts JM and Koff A. (1994). *Genes Dev.,* **8,** 9–22.
Reynisdottir I, Polyak K, Iavarone A and Massagué J. (1995). *Genes Dev.,* **9,** 1831–1845.
Roberts AB and Sporn MB. (1990). *Peptide Growth Factors and Their Receptors*. Springer: Heidelberg, pp. 421–472.
Sánchez A, Álvarez AM, Benito M and Fabregat I. (1996). *J. Biol. Chem.,* **271,** 7416–7422.
Schrantz N, Blanchard DA, Auffredou M, Sharma S, Leca G and Vazquez A. (1999). *Oncogene,* **18,** 3511–3519.
Sherr CJ and Roberts JM. (1999). *Genes Dev.,* **13,** 1501–1512.
Slingerland JM, Hengst L, Pan C, Alexander D, Stampfer MR and Reed SI. (1994). *Mol. Cell Biol.,* **14,** 3683–3694.
Tan X and Wang JY. (1998). *Trends Cell Biol.,* **8,** 116–120.
Tsubari M, Taipale J, Tiihomen E, Keski-Oja J and Laiho M. (1999). *Mol. Cell. Biol.,* **19,** 3654–3663.
Wang J and Walsh K. (1996). *Science,* **273,** 359–361.
Zhang Y, Fujita N and Tsuruo T. (1999). *Oncogene,* **18,** 1131–1138.
Zhou BB, Li H, Yuan J and Kirschner MW. (1998). *Proc. Natl. Acad. Sci. USA,* **95,** 6785–6790.